Geomechanics and Engineering, *Vol. 9, No. 5 (2015) 585-599*
DOI: http://dx.doi.org/10.12989/gae.2015.9.5.585

Experimental investigation of lateral displacement of PVD-improved deposit

Jin-Chun Chai and Fang Xu*

Department of Civil Engineering and Architecture, Saga University, Saga, Japan

(*Received October 16, 2014, Revised February 10, 2015, Accepted May 20, 2015*)

Abstract. Laboratory model tests were conducted to investigate the effect of surcharge loading rate on the magnitude of lateral displacement of prefabricated vertical drains (PVDs) improved deposit. The test results indicate that under the condition that the system had sufficient factor of safety (FS) (FS ≥ 1.2), for the similar model ground under the same total applied surcharge load, the lateral displacement increases with the increase of loading rate. The test results have been used to check the validity of a previously proposed method for predicting the maximum lateral displacement, and it shows that the data points are around the middle line of the predicted range, which supports the usefulness of the proposed method. The basic idea of the prediction method is an empirical relationship between the normalized lateral displacement (NLD) and a ration of load to the undrained shear strength of the deposit (RLS). The model test results offer some modifications of the NLD-RLS relationship: (1) instead of a bilinear relationship, NLD-RLS relationship may be entirely nonlinear; (2) the upper bound value of RLS for the proposed method can be used may be limited to 2.1 instead of the originally proposed value of 3.0.

Keywords: lateral displacement; prefabricated vertical drain; model test; embankment; soft deposit

1. Introduction

Demand for constructing embankments on soft clayey deposits in coastal regions increases with the development of modern transport infrastructures, such as highway, railway and airports. Prefabricated vertical drain (PVD) has been widely used in engineering practice to accelerate the consolidation process of clayey deposit (e.g., Asha and Mandal 2012, Rujikiatkamjorn *et al*. 2013, Parsa-Pajouh *et al*. 2014, Howell *et al*. 2014, Kim *et al*. 2014, Karim and Lo 2015). The embankment load not only induces vertical stresses but also shear stresses in the soft ground, and it induces settlements and lateral displacements of the ground. Predicting the embankment load induced ground deformation is one of the main issues considered in the design of an embankment on soft deposit. Generally, relative good agreements can be achieved between the predicted and measured settlements for the cases of embankment on PVD-improved deposit (e.g., Tan 1995, Tan and Chew 1996, Cascone and Biondi 2013, Hu *et al*. 2014). However, predicting the lateral displacement remains as a difficult task.

*Corresponding author, Ph.D. Student, E-mail: xufang.you@163.com

http://www.techno-press.org/?journal=gae&subpage=7 ISSN: 2005-307X (Print), 2092-6219 (Online)

For embankments constructed on natural clayey deposits, some empirical relationships between the maximum lateral displacement (δ_m) and the ground surface settlement on the embankment centerline (S_f) had been proposed (e.g., Tavenas and Leroueil 1980, Loganathan *et al*. 1993, Smadi 2001). These empirical methods provide simple statistics of the values of δ_m/S_f of the case of embankment on natural deposit without theoretical consideration of the main factors affecting lateral displacement. For the case of embankment on PVD-improved deposit, Ong and Chai (2011) and Chai *et al*. (2013) reported that the main factors affecting the lateral displacement are the embankment load, loading rate, embankment geometry, and the deformation, consolidation and strength of the subsoil. Chai *et al*. (2013) proposed a parameter (a ratio of load to the undrained shear strength of the deposit (RLS)) to include the effects of these main affecting factors. The ratio, δ_m/S_f, was designated as the normalized lateral displacement (NLD). Then based on available field data, a bilinear relationship between NLD and RLS for PVD-improved deposit under embankment loading with or without the application of vacuum pressure has been proposed by Xu and Chai (2014). For a given value of RLS, the predicted value of NLD has a bound width of 0.1, i.e., the range of the variation of δ_m is 10% of S_f.

To use the method for practical design, further verification and refinement are needed. Comparing with field cases, laboratory model tests can be conducted under controlled conditions and it provides a powerful tool for investigating the effect of the main influencing factors, such as the loading rate. And also, the results of well controlled model tests can provide a base for assessing the validity and usefulness of the existing prediction method.

In this study, large scale laboratory model tests were conducted to investigate the lateral displacement of PVD-improved deposit under embankment loading. The model tests were performed under different surcharge loading rate, while the total applied load was kept constant. The analyzed results of the test data indicated that the NLD-RLS relationship is located around the middle line of the bilinear range proposed by Chai *et al*. (2013) and Xu and Chai (2014) and the NLD-RLS relationship is nonlinear. Some modifications of the NLD-RLS relationship were also made.

2. Test device and materials

The test device used is illustrated in Figs. 1(a)-(b). It mainly consists of a metal box with inner dimensions of 1.50 m in length, 0.62 m in width and 0.85 m in height. The front and back walls of the box are made of transparent acrylic glass, which facilitated the direct observation of lateral displacement from outside. The model ground was divided into two parts by a 15 mm thick acrylic glass plate fixed at the center of the model box along the longitudinal direction. The surcharge (embankment) load was applied by air pressure through three Bellofram cylinders (diameter: 100 mm; maximum elongation: 140 mm) together with three metal loading plates with dimensions of 0.29 m in length, 0.166 m in width and 0.02 m in thickness. The soil used was remolded Ariake clay with liquid limit, w_L = 114.0%, plastic limit, w_P = 60.6%. The Mini-PVDs used to accelerate the consolidation process of the model ground were made of nonwoven geotextiles with a cross-section of 0.03 m × 0.01 m. And two piezometers (P_1 and P_2) were installed in the model ground to monitor the variations of the excess pore water pressure inside the model ground and their depths are indicated in Fig. 1(a). The settlements and pore water pressures were recorded using a computer linked to a data logger.

3. Test procedures

3.1 Preparation of model ground

Three layers of nonwoven geotextiles (thickness: 3 mm; weight: 130 g/m^2) were first placed at the bottom of the model box functioned as a bottom drainage layer. Then four flexible plastic strips for measuring the lateral displacement were lined vertically on the inner face of the front and back transparent acrylic glass walls. Initially several pieces of adhesive tape were applied to keep the plastic strips attached on the glass walls. Then thoroughly remolded Ariake clay slurry with water content of about 145% (about 1.3 w_L) or 125% (about 1.1 w_L) was filled in the model box layer by layer to reach a total thickness of about 0.8 m. When the surface of the soil reached the level where the tape used to fix the flexible plastic strips, the tapes were removed to allow the

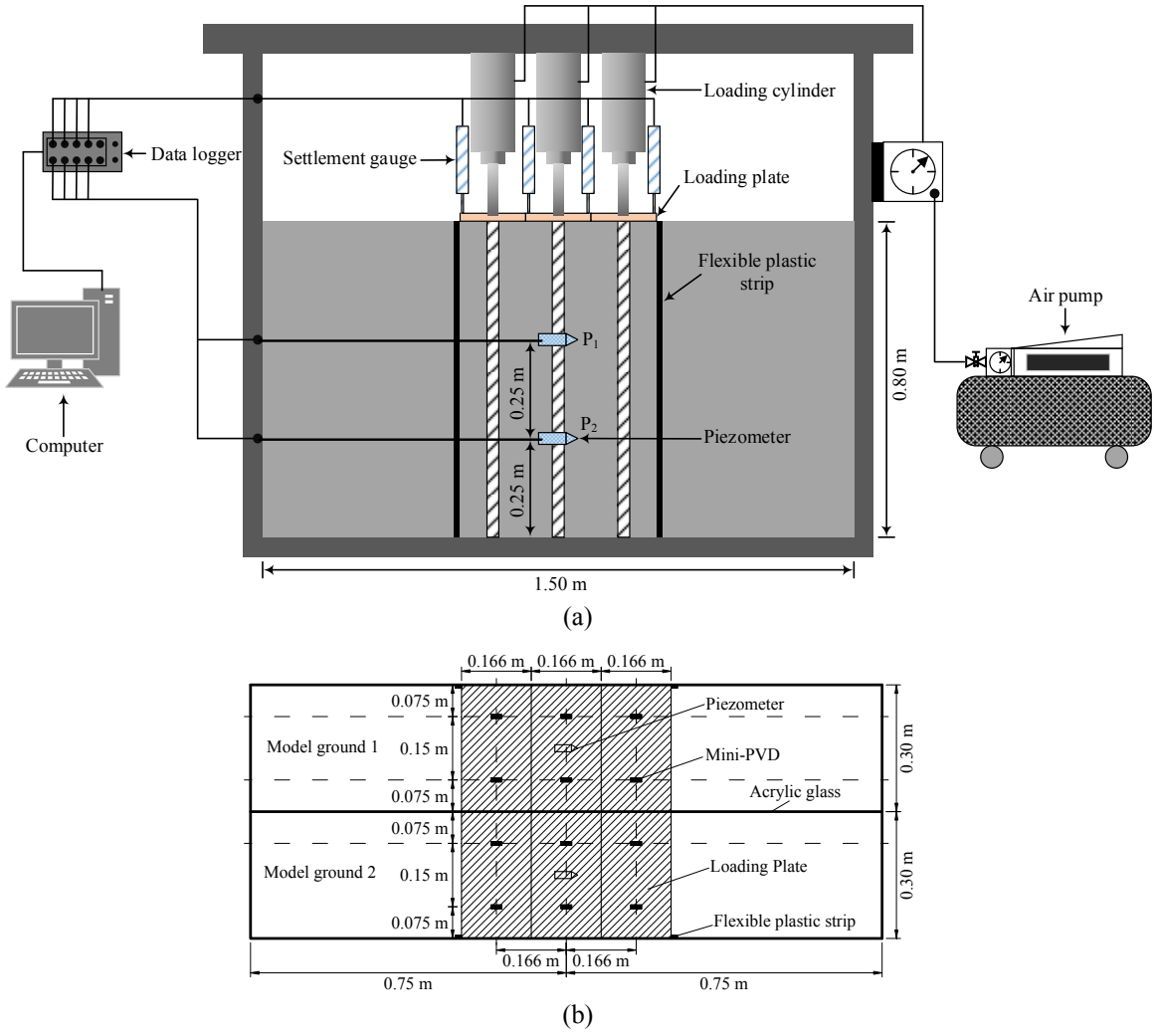

Fig. 1 Schematic diagram of laboratory model test: (a) cross section; (b) plan view

plastic strips to move with the soil during applying surcharge (embankment) load. During the filling process, two piezometers were installed at 0.25 m (P_2) and 0.50 m (P_1) from the bottom of the model ground. Finally, another three layers of nonwoven geotextiles were placed at the top surface of the model ground to act as a surface drainage layer.

The model ground was first pre-consolidated under a uniform pressure of 10 kPa by dead load under two-way drainage conditions for a duration of more than 60 days to reach a degree of consolidation of about 90%. After pre-consolidation the model ground was about 0.65 m thick. Then, the dead load was removed and two independent model grounds (length: 1.50 m; width: 0.30 m; thickness: 0.65 m) were formed. For each model ground two soil samples were taken from the soil near the left and right sides of the model box to conduct conventional oedometer consolidation tests.

3.2 Installation of mini-PVDs

Six mini-PVDs were driven into the model ground by a steel rod in a rectangular pattern of 0.166 m × 0.15 m as shown in Fig. 1(b). After the mini-PVDs fully penetrated into the model ground the steel rod was withdrawn and the mini-PVDs were left in the model ground.

3.3 Application of surcharge (embankment) load

Before applying the surcharge (embankment) load, four settlement gauges were settled on the loading plates (one on each loading plate at the two sides and two on the central loading plate) to measure the ground surface settlements. To simulate the embankment load, the pressure applied on the loading plates at the two sides was half of the value applied on the central one. The load was applied in a stepwise manner, i.e., increment loads were instantly applied with pre-determined time interval. During the tests, some tilting of the loading plates at the two sides was observed. When the tilting was large and influenced the firm contact between the loading rod and the loading plate, the load was temporarily released and some geotextiles were added below the loading plate at the larger settlement side to keep the plate almost horizontal, and the load was applied again.

4. Cases tested

The cases tested are summarized in Table 1. For all of the cases, the total applied surcharge load was the same of 60 kPa, while the loading rate was different. After the surcharge load reached the designed value of 60 kPa, it was maintained for a period of about two weeks before terminating the tests. After the test completed, soil samples at different depth were taken under the centerline of the surcharge loading area and their undrained shear strengths were measured by laboratory mini-vane shear tests. The mini-vane used was 20 mm in diameter and 40 mm in height, and the shearing speed was 6 degrees/min.

5. Test results

5.1 Settlement-time curves

The ground surface settlement curves measured at the central loading plate of Cases 1 to 6 are shown in Figs. 2-7, respectively. For Case 1, at about 33 days (3 days after the end of surcharge

load application) of the total elapsed time, there was an increase of the settlement rate, it was because before that time the piston of the central Bellofram cylinder reached its maximum

Table 1 Cases tested

Case	Surcharge load (kPa)	Loading rate (kPa/day)	w_n^* (%)
1	60	2	145
2	60	4	
3	60	6	125
4	60	8	
5	60	5	145
6	60	7	

*w_n = initial water content of the clay slurry used

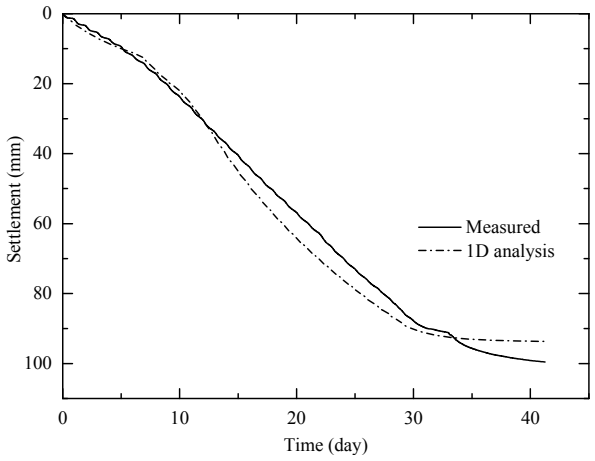

Fig. 2 Ground surface settlement of Case 1

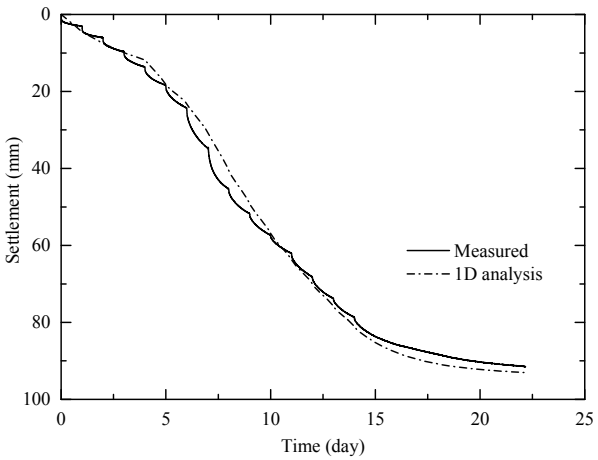

Fig. 3 Ground surface settlement of Case 2

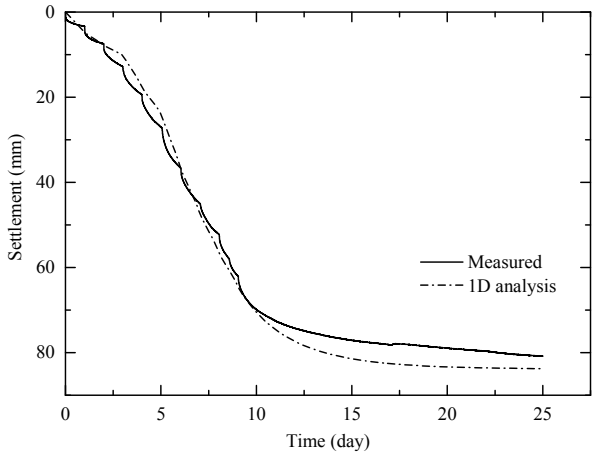

Fig. 4 Ground surface settlement of Case 3

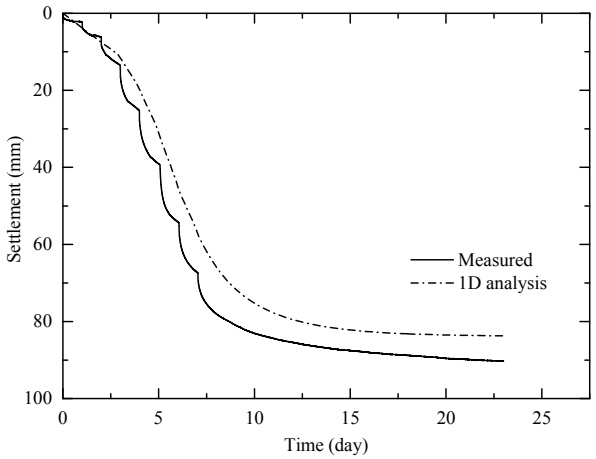

Fig. 5 Ground surface settlement of Case 4

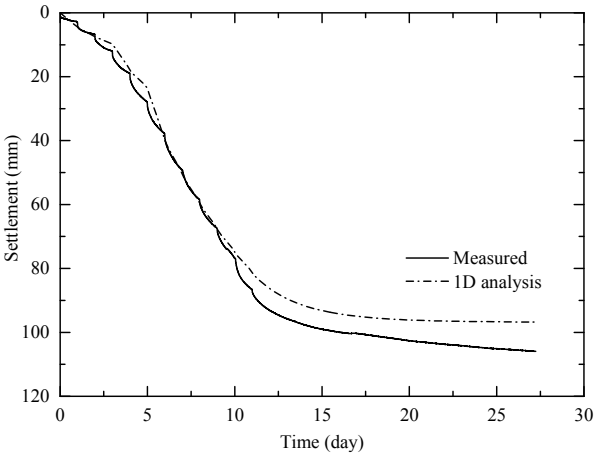

Fig. 6 Ground surface settlement of Case 5

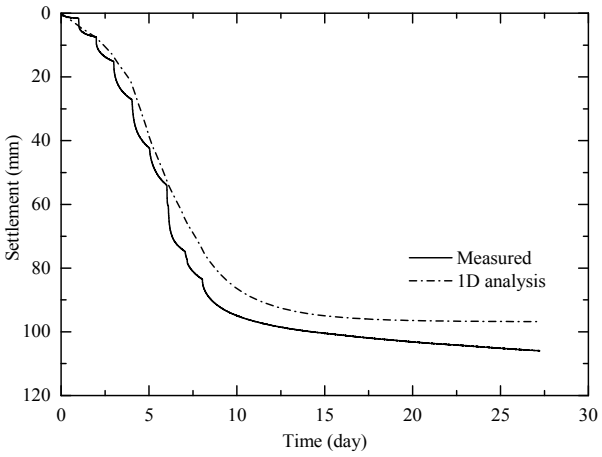

Fig. 7 Ground surface settlement of Case 6

elongation. The problem was solved by adding a metal block on the loading plate and the settlement rate increased immediately after that. For Case 6, the same issue as Case 1 was occurred at about 6 days of the total elapsed time. The model ground of Cases 1, 2, 5 and 6 had larger initial water content and resulted in larger settlements than that of Cases 3 and 4. Case 4 had larger settlement than that of Case 3. This difference was caused by the larger loading rate of Case 4 which induced larger lateral displacement. Generally, most of the lateral displacements are due to the undrained shear deformation. Under undrained condition, there is almost no volume change of the saturated subsoil, which implies that the settlement volume is almost equal to the lateral displacement volume in this stage. Therefore, the larger lateral displacement results in more ground settlement.

5.2 Lateral displacements

The final measured lateral displacements profiles under the edge of the surcharge loading area are plotted in Figs. 8-13 for Cases 1 to 6, respectively. For the same case, the measured lateral displacements at two edges of the loading area were not exactly identical. The similar phenomenon was reported for some field cases, such as Cowland and Wong (1993) and Kelln *et al*. (2007).

Figs. 8-13 clearly show that the loading rate had an obvious effect on the ground lateral displacement profile. For the similar model grounds, the larger the loading rate was, the larger the maximum lateral displacement. The model grounds of Cases 3 and 4 had lower initial water content, but due to the larger loading rate, the measured maximum lateral displacements were larger than those for Cases 1 and 2. Another interesting point is that comparing with Cases 1 and 2, the level where the maximum lateral displacement occurred was shallower for Cases 3 and 4. Although the exact reason is not clear, one possible reason is that with larger load rate, the stiffer surface layer due to the vertical drainage was thinner. For the consolidation due to vertical drainage, the soil just below the ground surface (drained boundary) consolidates much faster and gets stiffer than the soil locates at a certain depth below the ground surface. With increase of elapsed time, the effect of vertical consolidation will propagate into a deeper soil layer. For a faster load application, the thickness of the surface layer affected by the vertical drainage will be thinner.

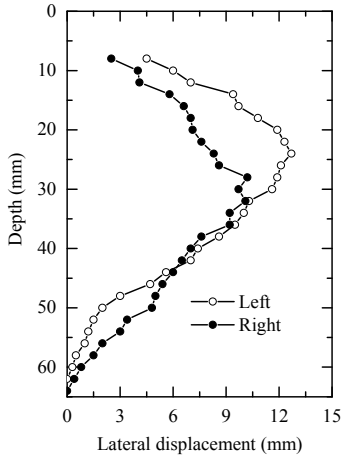

Fig. 8 Lateral displacement profile of Case 1

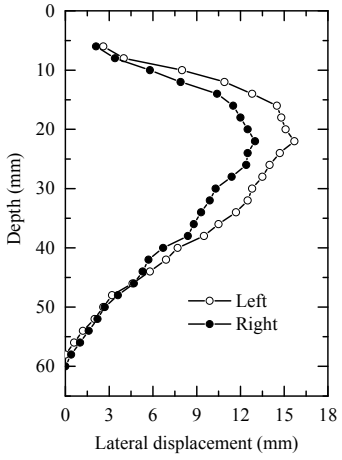

Fig. 9 Lateral displacement profile of Case 2

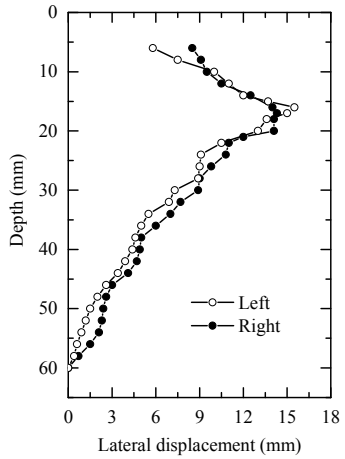

Fig. 10 Lateral displacement profile of Case 3

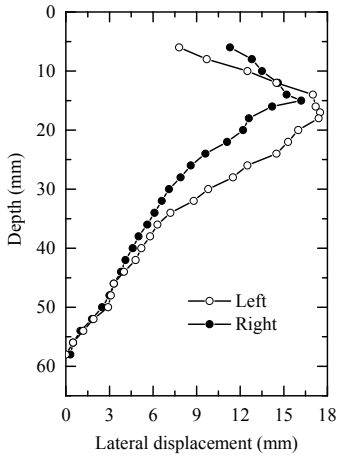

Fig. 11 Lateral displacement profile of Case 4

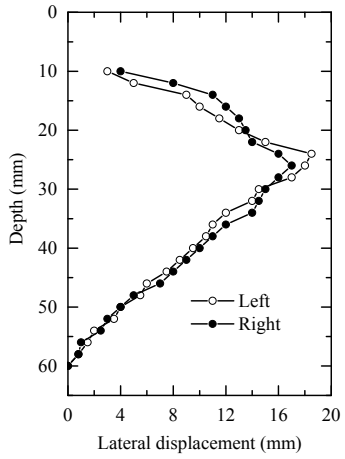

Fig. 12 Lateral displacement profile of Case 5

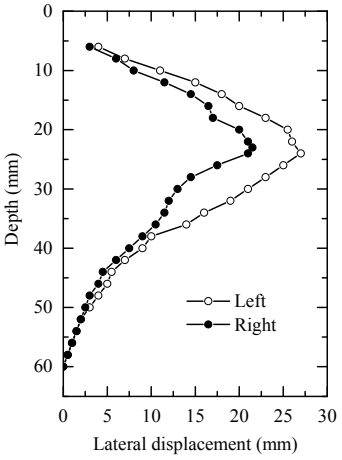

Fig. 13 Lateral displacement profile of Case 6

5.3 Variation of excess pore water pressure

Figs. 14-15 present the typical variations of the excess pore water pressure for Case 3 and Case 4, respectively. For Case 4, P_2 was malfunctioned, and the measurements were excluded. There was a clear trend of the excess pore water pressure increased when applying surcharge load and dissipated during consolidation period. At the initial stage of applying surcharge load (about 3 days of the total elapsed time) as well as the final stage, the measured excess pore water pressure was negative. There are two possible reasons. One is that the Mini-PVDs were dry before inserting them into the model grounds, and after inserted they would absorb water from the surrounding soil, therefore induced an initial suction pressure around the Mini-PVDs. The other one is that the bottom of the model ground was drained and the water pressure was zero which was less than the static water pressure, i.e., about 6 kPa suction pressure was applied at the bottom boundary.

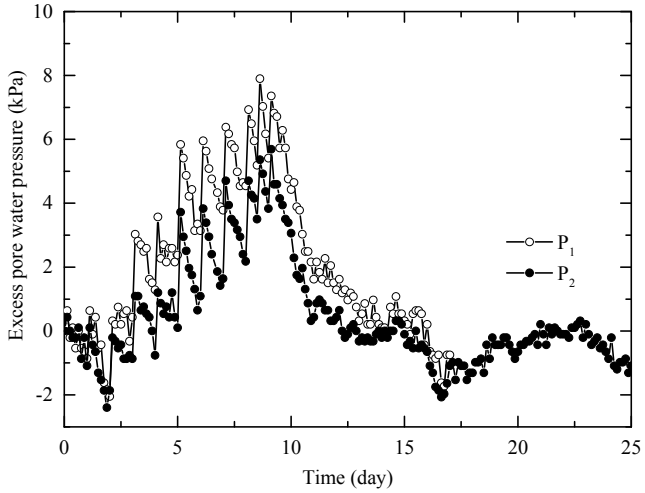

Fig. 14 Excess pore water pressure of Case 3

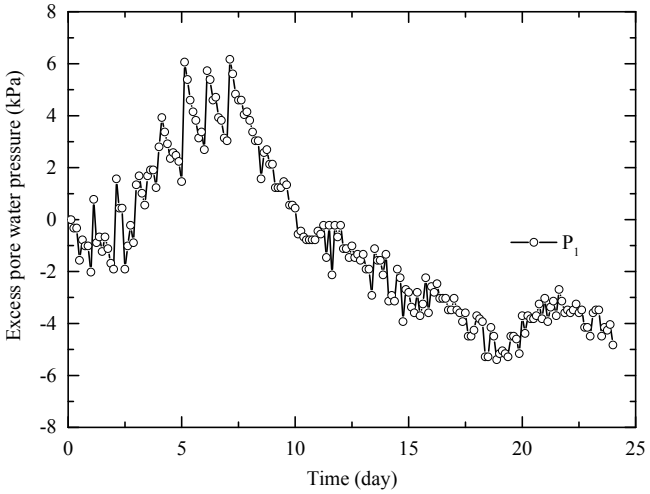

Fig. 15 Excess pore water pressure of Case 4

The loading rate of Case 4 was larger than that of Case 3, however the measured maximum excess pore water pressure was less than that of Case 3. The exact reason is not clear, possibly the piezometers were installed closer to the Mini-PVDs for Case 4.

6. Method for analyzing NLD-RLS relationship

Chai *et al*. (2013) and Xu and Chai (2014) proposed a method to predict the lateral displacement of PVD-improved deposit under embankment load with or without the application of vacuum pressure. The method is an empirical relationship between the normalized lateral displacement (NLD) and the ratio of an index pressure (p_n) to the representative undrained shear strength (s_u) of the soft subsoil (RLS). The method has been used to analyze the model test results. Some essence equations of the method are introduced below.

6.1 Definition of NLD

NLD is expressed as

$$\mathrm{NLD} = \frac{\delta_{nm}}{S_f} \tag{1}$$

where S_f is the final settlement of the ground surface on the embankment centerline, and δ_{nm} is the maximum net lateral displacement in the ground under the toe of the embankment. For the case of combining embankment load and vacuum pressure, δ_{nm} is the value of the maximum outward lateral displacement reduced by the maximum inward lateral displacement; while for the case of only embankment load, δ_{nm} is the maximum value of the outward lateral displacement. In design stage, S_f is calculated assuming one-dimensional (1D) consolidation deformation condition but considering the vertical stress spreading in the subsoil due to the embankment load by Osterberg (1957)'s method. For the model tests, the vertical stress spreading effect is considered by Boussinesq (1885)'s solution.

6.2 Definition of RLS

An index pressure (p_n) is expressed as

$$p_n = p_{em} - \left(\left|p_{vac}\right| + p_{em}\right)U \tag{2}$$

where p_{em} is the maximum value of the embankment load; p_{vac} is the vacuum pressure applied (for the case of only embankment load, p_{vac} is zero); and U is the average degree of consolidation of the PVD-improved zone corresponding to the end of embankment construction. U is calculated using Terzaghi's 1D consolidation theory for vertical drainage induced consolidation and using Hansbo (1981)'s solution for PVD induced consolidation. The detailed procedures can be found from Chai *et al*. (2013).

Then RLS is defined as

$$\mathrm{RLS} = \frac{p_n}{s_u} \tag{3}$$

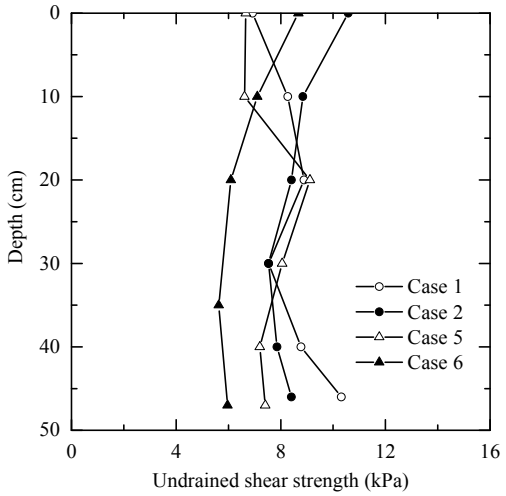

Fig. 16 Undrained shear strength profiles of Cases 1, 2, 5 and 6

where s_u is the representative undrained shear strength of the PVD-improved zone corresponding to the end of embankment construction.

6.3 Average value of s_u of PVD-improved zone

The value of s_u of each soil layer is evaluated using Ladd (1991)'s equation

$$s_u = S\sigma'_v(OCR)^m \tag{4}$$

where S and m are costants, σ'_v is the representative vertical effective stress in a soil layer corresponding to the end of embankment construction, and OCR is overconsolidation ratio. In this study, the adopted value of m is 0.75 (Ladd 1991). For Cases 1, 2, 5 and 6, s_u values of the model ground were measured using laboratory mini-vane shear tests, and the results are shown in Fig. 16. Using these test results, a value of S of 0.33 was back-calculated. And in Eq. (3), the average value of s_u weighted by the thickness of the soil layers of the PVD-improved zone is used. For Cases 3 and 4, after the completion of the consolidation test under the total applied load of 60 kPa, further load was applied before the final termination. The further loaded part is not indicated in this study, and the measured values of s_u are not corresponding to the total applied load of 60 kPa and are not shown in Fig. 16.

7. Results and discussion

The soil parameters of the six cases tested and the drainage parameters of the Mini-PVDs are listed in Tables 2 and 3, respectively. For the purpose of hand calculation, the model ground was divided into three layers. For the surface and the bottom layers, both the vertical and horizontal drainages need to be considered, and their thickness was 178 mm, the same as the diameter of the unit cell (mini-PVD and its improvement area) (Xu and Chai 2014), and for the middle layer, only horizontal drainage needs to be considered, and it was 294 mm thick. The analyzed settlements of

the six cases are compared with the measured data in Figs. 2-7 for Cases 1 to 6, respectively. The analyzed settlement curves were obtained by two steps analyses:

(1) the average degree of consolidation of the subsoil was calculated using Terzaghi's 1D and PVD consolidation theories considering stepwise loading (Chai and Miura 2002).

(2) the compression of the subsoil was calculated using 1D compression analysis considering the spreading of vertical stress in the model ground due to the surcharge load by Boussinesq (1885)'s solution.

Table 2 Parameters of the model ground soil

Case	γ_t (kN/m^3)	e_0	C_c (C_s/C_c)	k_v (m/day)	c_v (m^2/day)	p'_c (kPa)		
						Sur	Mid	Bot
Case 1 and 2	13.68	3.12	0.927 (0.1)	6.4×10^{-5}	1.7×10^{-3}	10	9.3	10
Case 3 and 4	14.03	2.82	0.774 (0.1)	5.3×10^{-5}	1.6×10^{-3}	10	9.4	10
Case 5 and 6	13.75	3.07	0.830 (0.1)	6.0×10^{-5}	1.65×10^{-3}	8	7.3	8
Ong-1	13.5	3.39	0.691 (0.1)	4.85×10^{-5}	8.1×10^{-4}		10	
Ong-2	13.5	3.39	0.691 (0.1)	4.85×10^{-5}	7.1×10^{-4}		10	

γ_t = total unit weight; e_0 = initial void ratio; C_c = compression index; C_s = swelling index; k_v = hydraulic conductivity in the vertical direction; c_v = coefficient of consolidation in the vertical direction; p'_c = pre-consolidation pressure. Sur = surface layer, thickness, 178 mm; Mid = middle layer, thickness, 294 mm; Bot = bottom layer, thickness, 178 mm

Table 3 Mini-PVD parameters

D_e (m)	d_w (m)	d_s (m)	k_h/k_s	q_w (m^3/day)	l (m)
0.178	0.02	0.08	1.6	1.0	0.65

D_e = diameter of unit cell (a mini-PVD and its improvement area); d_w = diameter of mini-PVD; d_s = diameter of smear zone; k_h = horizontal hydraulic conductivity of undisturbed zone; k_s = hydraulic conductivity of smear zone; q_w = discharge capacity of mini-PVD; l = drainage length

Table 4 Analyzed results of the cases tested

Case	U (%)	p_n (kPa)	s_u (kPa)	RLS	S_f (mm)	δ_m-left (mm)	δ_m-right (mm)	NLD -left	NLD -right
Case 1	94.5	3.3	11.2	0.295	99.5	12.7	10.2	0.128	0.103
Case 2	87.4	7.6	10.4	0.727	91.5	15.7	13.0	0.172	0.142
Case 3	79.0	12.6	9.5	1.326	80.8	15.5	14.3	0.192	0.177
Case 4	72.7	16.4	8.8	1.861	90.3	17.5	16.2	0.194	0.179
Case 5	83.1	10.1	9.9	1.024	105.9	18.5	17.0	0.175	0.161
Case 6	76.6	14.0	9.2	1.526	106.0	27.0	21.5	0.255	0.203
Ong-1	59.1	6.8	12.8	0.532	77.0	12.0	—	0.156	—
Ong-2	48.8	-3.9	12.0	-0.327	98.0	-2.0	1	-0.020	-0.010

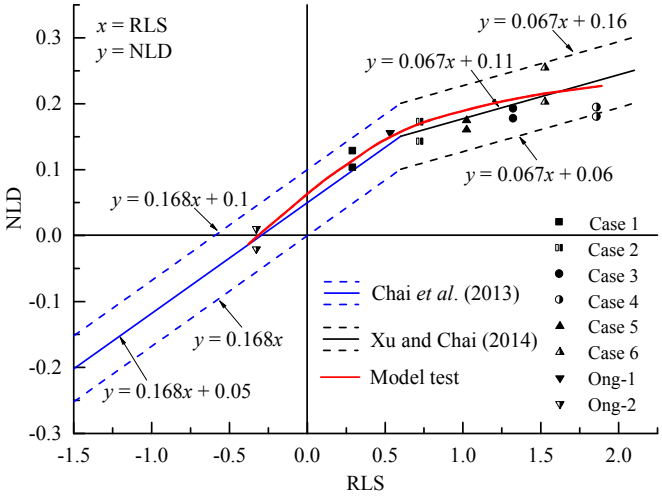

Fig. 17 Analyzed NLD-RLS relationship from test results

It is shown that the analyzed results agreed well with the measured data. Then the calculated values of U, p_n, s_u, NLD and RLS and the final measured maximum lateral displacement (δ_m) and the ground surface settlement (S_f) on the embankment centerline are listed in Table 4. It can be seen that for the similar model ground (e.g., Case 1 and Case 2) under the same total surcharge load, the value of NLD increases with the increase of loading rate.

Ong (2011) reported some similar model tests but under the combination of surcharge and vacuum pressure loadings. Two cases from Ong (2011) (Ong-1 and Ong-2) were analyzed. The model ground parameters are given in Table 2 and the analyzed results are listed in Table 4 also.

The results (NLD and RLS) in Table 4 are plotted in Fig. 17 together with the proposed NLD-RLS relationships for the combined embankment loading and vacuum pressure loading by Chai *et al*. (2013) and embankment loading alone by Xu and Chai (2014). It can be seen that the model test results are around the middle line of the proposed range, which provides a strong support for the validity of the proposed relationship based on the field data. However, the model test results indicated that the NLD-RLS relationship may not be a straight line, but curved, i.e., NLD is not linearly increase with the increase of RLS. In case the embankment has sufficient factor of safety (FS ≥ 1.2), the increase rate of NLD reduces with the increase of RLS. The reason is that with the increase of the maximum lateral displacement, the constraining effects from the soil layers above and below the level where the maximum lateral displacement occurs will increase, which tends to restrain the further development of the maximum lateral displacement. When Xu and Chai (2014) proposed the NLD-RLS relationship for the only embankment loading cases, there is only one data point for RLS > 2.1. A model test was conducted with a larger loading rate, but it was failed before the planed total load of 60 kPa was applied. Based on the model test results and considering the factor of only one (1) data point for RLS > 2.1, it is suggested to limit the upper bound of RLS to 2.1 instead of the originally proposed value of 3.0.

8. Conclusions

Well controlled large scale laboratory model tests were conducted to investigate the behavior of

lateral displacement of prefabricated vertical drains (PVDs) improved soft deposit under embankment (surcharge) loading. The main factor investigated is the surcharge loading rate. The test results indicate that the maximum lateral displacement increases with the increase of loading rate.

The results of the model tests in this study together with the results of another two existing tests under the combination of embankment and vacuum pressure loadings were analyzed using the normalized lateral displacement (NLD) and the ratio of an index load to the undrained shear strength of the soft subsoil (RLS). The analyzed results are located around the middle line of the predicted range of the NLD-RLS relationship derived based on filed data, which provides a strong support for the usefulness of the proposed method.

The model test results also provide some modifications of the prediction method. Instead of a bilinear relationship, the NLD-RLS relationship is nonlinear. And the upper bound value of RLS for the proposed method to be valid may be limited to 2.1 instead of the originally proposed value of 3.0.

References

Asha, B. and Mandal, J. (2012), "Absorption and discharge capacity tests on natural prefabricated vertical drains", *Geosynth. Int.*, **19**(4), 263-271.

Boussinesq, J. (1885), *Application des Potentials à L'Etude de L'Équilibre et du Mouvement des Solides Élastiques*, Gauthier-Villars, Paris, France. [In French]

Cascone, E. and Biondi, G. (2013), "A case study on soil settlements induced by preloading and vertical drains", *Geotext. Geomembr.*, **38**, 51-67.

Chai, J.-C. and Miura, N. (2002), "Long-term transmissivity of geotextile confined in clay", *Proceedings of the 7th International Conference on Geosynthetics*, Nice, France, Volume 1, September, pp. 155-158.

Chai, J.-C., Ong, C.Y., Bergado, D.T. and Carter, J.P. (2013), "Lateral displacement under combined vacuum pressure and embankment loading", *Géotechnique*, **63**(10), 842-856.

Cowland, J. and Wong, S. (1993), "Performance of a road embankment on soft clay supported on a geocell mattress foundation", *Geotext. Geomembr.*, **12**(8), 687-705.

Hansbo, S. (1981), "Consolidation of fine-grained soils by prefabricated drains", *Proceedings of the 10th International Conference on Soil Mechanics and Foundation Engineering*, Stockholm, Sweden, June, Volume 3, pp. 677-682.

Howell, R., Rathje, E. and Boulanger, R. (2014), "Evaluation of simulation models of lateral spread sites treated with prefabricated vertical drains", *J. Geotech. Geoenviron. Eng.*, **141**(1), 04014076.

Hu, Y., Zhou, W.-H. and Cai, Y. (2014), "Large-strain elastic visco-plastic consolidation analysis of very soft clay layers with vertical drains under preloading", *Can. Geotech. J.*, **51**(2), 144-157.

Karim, M.R. and Lo, S.-C. (2015), "Estimation of the hydraulic conductivity of soils improved with vertical drains", *Comput. Geotech.*, **63**, 299-305.

Kelln, C., Sharma, J., Hughes, D. and Gallagher, G. (2007), "Deformation of a soft estuarine deposit under a geotextile reinforced embankment", *Can. Geotech. J.*, **44**(5), 603-617.

Kim, H.J., Lee, K.H., Jamin, J.C. and Mission, J.L.C. (2014), "Stochastic cost optimization of ground improvement with prefabricated vertical drains and surcharge preloading", *Geomech. Eng., Int. J.*, **7**(5), 525-537.

Ladd, C.C. (1991), "Stability evaluation during staged construction", *J. Geotech. Eng. ASCE*, **117**(4), 540-615.

Loganathan, N., Balasubramaniam, A.S. and Bergado, D.T. (1993), "Deformation analysis of embankments". *J. Geotech. Eng. ASCE*, **119**(8), 1185-1206.

Ong, C.Y. and Chai, J.-C. (2011), "Lateral displacement of soft ground under vacuum pressure and

surcharge load", *Front. Arch. Civil Eng. China*, **5**(2), 239-248.
Ong, C.Y. (2011), "Prediction of lateral displacement of ground induced by surcharge load and vacuum pressure", Ph.D. Dissertation; Saga University, Saga, Japan.
Osterberg, J.O. (1957), "Influence values for vertical stresses in a semi-infinite mass due to an embankment loading", *Proceedings of the 4th Intornational Conference Soil Mechanics and Foundation Engineering*, London, UK, August ,Volume 1, pp. 393-394.
Parsa-Pajouh, A., Fatahi, B., Vincent, P. and Khabbaz, H. (2014), "Analyzing consolidation data to predict smear zone characteristics induced by vertical drain installation for soft soil improvement", *Geomech. Eng., Int. J.*, **7**(1), 105-131.
Rujikiatkamjorn, C., Ardana, M., Indraratna, B. and Leroueil, S. (2013), "Conceptual model describing smear zone caused by mandrel action", *Géotechnique*, **63**(16), 1377-1388.
Smadi, M.M. (2001), "Lateral deformation and associated settlement resulting from embankment loading of soft clay and silt deposits", Ph.D. Dissertation; University of Illinois, Urbana-Champaign, IL, USA.
Tan, S.A. (1995), "Validation of hyperbolic method for settlement in clays with vertical drains", *Soils Found.*, **35**(1), 101-113.
Tan, S.-A. and Chew, S.-H. (1996), "Comparison of the hyperbolic and Asaoka observational method of monitoring consolidation with vertical drains", *Soils Found.*, **36**(3), 31-42.
Tavenas, F. and Leroueil, S. (1980), "The behaviour of embankments on clay foundations", *Can. Geotech. J.*, **17**(2), 236-260.
Xu, F. and Chai, J-C. (2014), "Lateral displacement of PVD-improved deposit under embankment loading", *Geosynth. Int.*, **21**(5), 286-300.

CC